ORIGINAL RESEARCH

Noninvasive MRI Monitoring of the Effect of Interventions on Endothelial Permeability in Murine Atherosclerosis Using an Albumin-Binding Contrast Agent

Alkystis Phinikaridou, PhD;* Marcelo E. Andia, MD, PhD;* Gabriella Passacquale, MD, PhD; Albert Ferro, FRCP, PhD; René M. Botnar, PhD

***Background*—**Endothelial dysfunction promotes atherosclerosis. We investigated whether in vivo magnetic resonance imaging (MRI) using an albumin-binding contrast agent, gadofosveset, could monitor the efficacy of minocycline and ebselen in reducing endothelial permeability and atherosclerotic burden in the brachiocephalic artery of high-fat diet (HFD)–fed ApoE$^{-/-}$ mice.

***Methods and Results*—**ApoE$^{-/-}$ mice were scanned 12 weeks after commencement of either a normal diet (controls) or an HFD. HFD-fed ApoE$^{-/-}$ mice were either untreated or treated with minocycline or ebselen for 12 weeks. Delayed-enhancement MRI and T_1 mapping of the brachiocephalic artery, 30 minutes after injection of gadofosveset, showed increased vessel wall enhancement and relaxation rate (R_1, s^{-1}) in untreated HFD-fed ApoE$^{-/-}$ mice (R_1=3.8±0.52 s^{-1}) compared with controls (R_1=2.15±0.34 s^{-1}, P<0.001). Conversely, minocycline-treated (R_1=2.7±0.17 s^{-1}, P<0.001) and ebselen-treated (R_1=2.7±0.23 s^{-1}, P<0.001) ApoE$^{-/-}$ mice showed less vessel wall enhancement compared with untreated HFD-fed ApoE$^{-/-}$ mice. Mass spectroscopy showed a lower gadolinium concentration in the brachiocephalic artery of treated (minocycline=28.5±3 μmol/L, ebselen=32.4±4 μmol/L) compared with untreated HFD-fed ApoE$^{-/-}$ mice (191±4.8 μmol/L) (P<0.02). Both interventions resulted in a lower plaque burden as measured by delayed-enhancement MRI (minocycline=0.14±0.02 mm^2, ebselen=0.20±0.09 mm^2, untreated=0.44±0.01 mm^2; P<0.001) and histology (minocycline=0.13±0.05 mm^2, ebselen=0.18±0.02 mm^2, untreated=0.32±0.04 mm^2; P<0.002). Endothelium cells displayed fewer structural changes and smaller gap junction width in treated compared with untreated animals as seen by electron microscopy (minocycline=42.3±8.4 nm, ebselen=56.5±17 nm, untreated=2400±39 nm; P<0.001). Tissue flow cytometry of the brachiocephalic artery showed lower monocyte/macrophage content in both ebselen- and minocycline-treated mice (8.06±3.2% and 7.62±1.73%, respectively) compared with untreated animals (20.1±2.2%) (P=0.03), with significant attenuation of the proinflammatory Ly6C^{high} subtype (untreated mice, 42.64±6.1% of total monocytes; ebselen, 14.07±9.5% of total monocytes; minocycline, 26.42±0.6% of total monocytes).

***Conclusions*—**We demonstrate that contrast-enhanced MRI with an albumin-binding contrast agent can be used to noninvasively monitor the effect of interventions on endothelial permeability and plaque burden. Blood albumin leakage could be a surrogate marker for the in vivo evaluation of interventions that aim at restoring endothelial integrity. **(*J Am Heart Assoc.* 2013;2:e000402 doi: 10.1161/JAHA.113.000402)**

Key Words: atherosclerosis • endothelial dysfunction • gadofosveset • monocytes • MRI • permeability

From the Division of Imaging Science and Biomedical Engineering (A.P., M.E.A., R.M.B.), Department of Vascular Biology (G.P., A.F.) and Cardiovascular Division, Wellcome Trust and EPSRC Medical Engineering Center (R.M.B.), King's College London, London, United Kingdom; Cardiovascular Division, BHF Centre of Excellence, King's College London, London, United Kingdom (A.P., G.P., A.F., R.M.B.); Radiology Department, School of Medicine, Pontificia Universidad Catolica de Chile, Santiago, Chile (M.E.A.).

The views expressed are those of the authors, and not necessarily those of the NHS, the NIHR, or the Department of Health.

*Drs Phinikaridou and Andia contributed equally to this article.

Correspondence to: Alkystis Phinikaridou, PhD, Division of Imaging Sciences and Biomedical Engineering, The Rayne Institute, King's College London, 4th Floor, Lambeth Wing, St Thomas' Hospital, London SE1 7EH, United Kingdom. E-mail: alkystis.1.phinikaridou@kcl.ac.uk

Received July 8, 2013; accepted August 2, 2013.

Atherosclerosis is a chronic disease of the vessels and a major cause of morbidity and mortality in Western societies and developing countries. Dysfunction of the vascular endothelium promotes atherosclerosis through leukocyte and monocyte arterial infiltration, platelet activation, and smooth muscle cell proliferation.[1] In addition, damaged endothelium can promote vasospasm and thrombosis, causing acute cardiovascular events.[1] Therefore, testing of treatments that could restore/improve endothelial function and reduce endothelial permeability may be beneficial in reducing atherosclerotic risk.

Magnetic resonance imaging (MRI) is a noninvasive imaging modality that offers high spatial resolution for the morphological and compositional evaluation of the vessel wall.[2–13] However, noninvasive MRI assessment of endothelial

permeability[14] and function[15–17] has only recently been achieved. Gadofosveset is a clinically approved gadolinium-based contrast agent that reversibly binds to serum albumin, resulting in a prolonged vascular presence and a 5-fold to 10-fold increase in relaxivity (r1).[18,19] Although, gadofosveset is a blood-pool agent, it may enter the vasculature through leaky neovessels[20,21] and damaged endothelium.[14] We have recently demonstrated that gadofosveset-enhanced MRI allowed noninvasive visualization and quantification of endothelial permeability in the brachiocephalic artery of high-fat diet (HFD)–fed ApoE$^{-/-}$ mice. Contrast uptake correlated with endothelial cell damage, widening of the gap junctions, and plaque burden.[22] Moreover, treatment of mice with statins showed less endothelial damage and plaque development. We thus postulated that statins might have a 2-fold effect—first, lowering total cholesterol levels, and second, having an anti-inflammatory effect. In the current work, we aimed to study the effect of 2 other interventions, ebselen (antioxidant) and minocycline (antibiotic), which belong to completely different drug classes, and we focused on their effects on endothelial integrity and plaque development.

Ebselen is a lipid-soluble low-molecular-weight seleno-organic compound and a known glutathione peroxidase-1 mimetic. Ebselen acts by reducing lipid hydroperoxides and scavenging peroxyl radicals. Ebselen has been shown to improve endothelial function and reduce atherosclerotic burden in different animal models[23,24] and myocardial infarct size in rabbits.[25] Minocycline is a tetracycline derivate with vasculoprotective effects independent of its antimicrobial properties. Minocycline reduced neointima formation following vascular injury of the rat carotid artery[26] and plaque metalloproteinase (MMP) activity promoting plaque stabilization.[27] Recently, it was shown that minocycline reduced plaque size and inhibited proliferation of vascular smooth muscle cells through a PARP-1- and p27^{Kip1}-dependent mechanism in ApoE$^{-/-}$ mice.[28]

In addition to endothelial dysfunction, inflammation is another hallmark of atherosclerosis. Monocytes are major cell components of the innate immune system that accumulate quickly in response to injury or infection. Circulating monocytes can be divided into 2 subsets, namely, 6C^{high} and Ly6C^{low} cells.[29] In mice, Ly-6C^{high} monocytes were shown to be potent inflammatory mediators,[29,30] whereas Ly-6C^{low} monocytes were shown to exhibit "patrolling" behavior[31] and may be important in the resolution of inflammation.[32] Hypercholesterolemic mice gradually accumulate Ly-6C^{high} monocytes in blood and developing lesions.[33,34] Ly-6C^{high} monocytes adhere to the activated endothelium, differentiate to macrophages within the developing plaque, and contribute to inflammation.[33,35–37] Although Ly-6C^{low} monocytes increase less severely, they take up oxidized low-density lipoprotein and likely differentiate into dendritic cells on tissue infiltration.[38,39]

Considering that minocycline and ebselen have atheroprotective effects, we investigated the effects of these interventions on: (1) endothelial permeability and plaque burden, using gadofosveset-enhanced noninvasive MRI methods that we have previously developed; and (2) on plaque inflammation as assessed by flow-cytometry analysis of plaque monocyte/macrophage infiltration.

Materials and Methods

Animals

Homozygous male ApoE$^{-/-}$ mice (B6.129P2–ApoE^{tm1Unc}/J) were purchased from Charles Rivers Laboratories (Edinburgh, UK). Eight-week-old ApoE$^{-/-}$ mice were fed either a normal chow diet and used as controls (n=6) or were switched to an HFD containing 21% fat from lard and 0.15% (wt/wt) cholesterol (Special Diets Services, Witham, UK) for 12 weeks. HFD-fed ApoE$^{-/-}$ mice were either left untreated (n=6) or treated with ebselen (n=6; 5 mg/kg body weight dissolved in 5% CM-cellulose; Sigma, Aldrich)[23,24] or minocycline (n=6; 1.5 mg/kg; PL Holder, Generic, UK).[27] Ebselen was administered by daily gavage, and minocycline was administered in the drinking water concurrently with the HFD for 12 weeks. All mice were imaged at the end of the 12-week period. All procedures used in these studies were licensed under the United Kingdom Animal (Scientific Procedures) Act 1986.

MRI Protocol

In vivo vessel wall imaging was performed using a 3T Philips Achieva MR scanner (Philips Healthcare, Best, The Netherlands) equipped with a clinical gradient system (30 mT/m, 200 mT/m per millisecond) and a single-loop surface coil (diameter, 23 mm) as previously described.[22] Briefly, anesthetized mice were imaged in the prone position before and 30 minutes after intravenous administration of 0.03 mmol/kg gadofosveset (Ablavar, Lantheus Medical Imaging, North Billerica). Following a 3D GRE scout scan, time-of-flight images were acquired for visualization of the aortic arch and the brachiocephalic and carotid arteries and for planning of the subsequent scans. A 2D-Look-Locker sequence was used to determine the optimal inversion time for blood signal nulling. An inversion-recovery 3D fast-gradient echo sequence was acquired 30 minutes postinjection and was used for visualization of contrast uptake. Imaging parameters were FOV, 30×30×8 mm; matrix, 304×304; resolution, 0.1×0.1 mm; measured slice thickness, 0.5 mm; slices, 32; TR/TE, 28/8 ms; TR between subsequent IR pulses, 1000 ms; and flip angle, 30°. T_1 mapping was performed using 2 nonselective inversion pulses with inversion times ranging from 20 to 3000 ms, followed by 8 segmented

readouts.[40] Images were acquired with FOV, 36×22×8 mm; matrix, 192×102; in-plane resolution, 0.18×0.22 mm; measured slice thickness, 0.5 mm; slices, 16; TR/TE, 9.6/4.9 ms; and flip angle, 10°.

MRI Image Analysis

Vessel wall area was calculated by manually segmenting the visually enhanced region of the vessel wall as seen on the delayed-enhancement (DE) MRI images using OsiriX (OsiriX Foundation, Geneva, Switzerland), and T_1 values were computed on a pixel-by-pixel basis using in-house Matlab software (Mathworks, Natick, MA) as previously described.[22]

Tissue Flow Cytometry

Immediately after collection, the brachiocephalic artery was microdissected and digested at 37°C for 1 hour in an enzymatic cocktail containing 125 U/mL collagenase type XI, 60 U/mL hyaluronidase type I-s, 60 U/mL DNase 1, and 450 U/mL collagenase type 1 (Sigma-Aldrich) in PBS supplemented with 20 mmol/L Hepes.[20] The artery was then mashed through a 70-μm strainer to obtain a cell suspension. The latter was resuspended in PBS supplemented with 0.2% BSA and incubated at 4°C for 20 minutes with a combination of the following antibodies: Per-CP anti-mouse lymphocyte markers (Lin) including B220, CD90, Ly6G, and NK1.1; APC anti-mouse F4/80; FITC anti-mouse CD115; and PE anti–mouse Ly-6C or CD11b (all antibodies were from eBiosciences, apart from the antimouse B220, which was purchased from Becton & Dickinson). A total of 50 000 events were acquired and on postacquisition analysis performed using FlowJo software (Tree Star, Ashland, OR); monocytes/macrophages were identified as a $CD11b^{high}$ $F4/80^{+}$ $CD115^{+}$ Lin^{-} (B220, CD90, Ly6G, NK1.1) population[41] and reported as percentage of cells per artery. Ly6C staining identified $Ly\text{-}6C^{high}$ and $Ly\text{-}6C^{low}$ subsets within the monocytic population. The percentage of each subset over total monocytes/macrophages is reported.

Histology

Tissue harvesting

Anesthetized mice were perfused through the left ventricle with physiological saline (electron microscopy studies) or formalin (standard histology) for 10 minutes and subsequently were euthanized.

Transmission electron microscopy

Brachiocephalic and left carotid arteries (n=2 per group) were pinned down and fixed in 2% glutaraldehyde in 0.1 mol/L sodium phosphate buffer (pH 7.4) for 2 hours, washed with sodium phosphate buffer for 2 hours, and postfixed in 1% OsO_4 for 2 hours. Samples were dehydrated and embedded in epoxy resin. Semithin sections (0.2 μm) were stained with toluidine blue for light microscopy examinations and were used to guide sampling for transmission electron microscopy studies. Sections (0.09 μm) were collected on 150 mesh copper grids and double-stained with uranyl acetate and lead citrate for electron microscopy examinations (H7650, Hitachi, Tokyo, Japan). Gap junction width was measured on electron microscopy sections cut perpendicular to the long axis of the vessel wall using ImageJ (NIH) as previously described.[22]

Inductively coupled mass spectrometry

Gadolinium concentrations of the vessel wall were determined by inductively coupled mass mass spectrometry (ICP-MS) as previously described.[22] Briefly, the brachiocephalic artery was collected and snap-frozen in liquid nitrogen (n=2 per group). Prior to ICP-MS, the samples were digested in 300 μL of 70% nitric acid overnight at room temperature, followed by dilution in 1 mL of deionized water. Gadolinium concentrations were normalized to the weight of the tissue.

Statistical Analysis

The Statistical Package for the Social Sciences 18.0 (SPSS Inc, Chicago, IL) was used. For multiple-group analysis, statistical comparisons were performed by 1-way analysis of variance followed by the Bonferroni post hoc test for analyzing the MRI measurements (R_1 and delayed area of enhancement when sample size=6). For analysis of ICP, flow cytometry, and histological data, the Kruskal–Wallis test followed by a Dunn's post hoc test was used because of the small sample size (n=2). Correlation analysis was performed using Spearman correlation. Intra- and interobserver variability for the segmentation of the vessel wall on MRI images was performed using intraclass correlation analysis based on a random-effects model. The data are presented as the mean±SD. $P<0.05$ was used to define statistical significance.

Results

Treatment With Minocycline and Ebselen Reduced Endothelial Permeability, Plaque Burden, and Gadofosveset Uptake

On postcontrast DE-MRI, greater enhancement of the brachiocephalic artery of $ApoE^{-/-}$ mice exposed to HFD for 12 weeks was observed compared with control mice (Figure $1A_{1\text{-}3}$ and $1B_{1\text{-}3}$). Conversely, mice treated with ebselen and minocycline showed decreased vessel wall enhancement

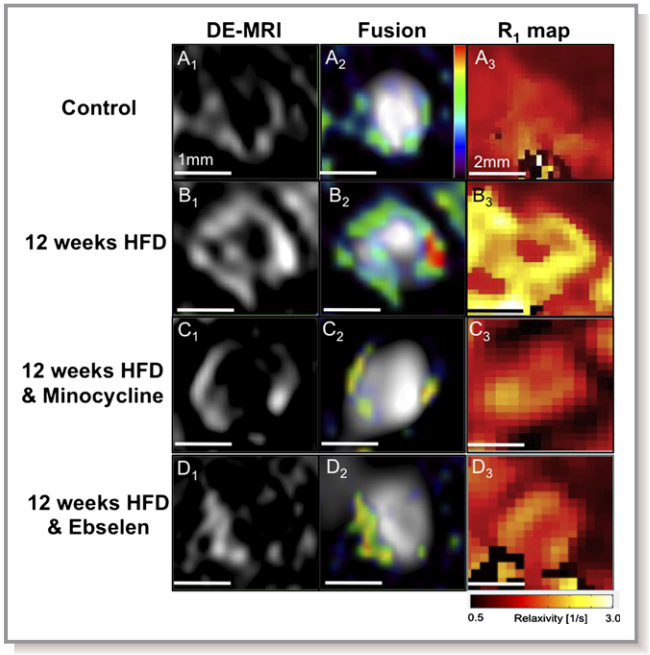

Figure 1. Treatment with minocycline and ebselen reduced endothelial permeability, plaque burden, and gadofosveset uptake. A_1 through D_1 and A_2 through D_2, Cross-sectional DE-MRI and DE-MRI fused with MRA images of the brachiocephalic artery. ApoE$^{-/-}$ mice on an HFD showed increased vessel wall enhancement corresponding to plaque progression, whereas minocycline- and ebselen-treated ApoE$^{-/-}$ mice showed less enhancement. A_3 through D_3, Corresponding R_1 maps quantify the amount of gadofosveset within the vessel wall. Intense yellow signal indicates increased gadofosveset concentration. DE-MRI indicates delayed-enhancement magnetic resonance imaging; HFD, high-fat diet; MRA, magnetic resonance angiography.

compared with untreated animals. Vessel wall gadolinium uptake was quantified using relaxation rate (R_1) maps (Figure 1A_3 through 1D_3; yellow coloration indicates a high R_1).

En face images (Figure 2A through 2C) and toluidine blue–stained cross sections (Figure 2D through 2F) illustrate the reduction of plaque burden in the brachiocephalic artery of treated compared with untreated ApoE$^{-/-}$ mice.

Quantitative MRI and Histological Analysis

Quantitative analysis of R_1 showed a significant increase in R_1 in atherosclerotic HFD-fed ApoE$^{-/-}$ (R_1=3.8±0.52 s^{-1}) compared with control (R_1=2.15±0.34 s^{-1}) mice (Figure 3A). Conversely, treatment with ebselen (R_1=2.7±0.23 s^{-1}) and minocycline (R_1=2.7±0.17 s^{-1}) significantly reduced the leakage of gadofosveset into the vessel wall and thus decreased the vessel wall R_1, compared with 12-week HFD-untreated ApoE$^{-/-}$ mice (P<0.001). These findings were corroborated by quantitation of the gadolinium concentration within the arterial wall by ICP-MS (minocycline-treated=28.5±3 μmol/L, ebselen-treated=32.4±4 μmol/L, untreated=191±4.8 μmol/L; P<0.02; Figure 3B). The changes in the contrast-enhanced area as measured on DE-MRI (minocycline=0.14±0.02 mm^2, ebselen=0.20±0.09 mm^2, untreated=0.44±0.01 mm^2; P<0.001; Figure 3C) and the plaque burden as measured by histology (minocycline=0.13±0.05 mm^2, ebselen=0.18±0.02 mm^2, untreated=0.32±0.04 mm^2; P<0.002; Figure 3D) showed a decrease in the contrast uptake and plaque burden when ApoE$^{-/-}$ mice were treated with minocycline and ebselen compared with the untreated group. Pearson correlation showed a significant positive correlation (r=0.58, P<0.03) between the plaque burden area calculated using DE-MRI images and corresponding histology. Our data showed good intraobserver (α=0.76; 95% CI, 0.48 to 0.89) and interobserver variability (α=0.75; 95% CI, 0.25 to 0.92) for segmenting the vessel wall on MRI images.

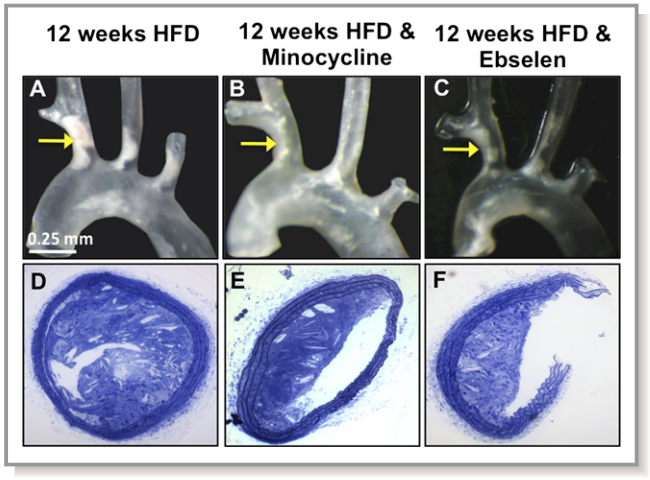

Figure 2. Treatment with minocycline and ebselen reduced plaque burden. A through C, En face images (A through C) and toluidine blue–stained cross-sections (D through F) illustrate the reduction of plaque burden in the brachiocephalic artery of treated ApoE$^{-/-}$ mice compared with untreated mice. HFD indicates high-fat diet.

Treatment With Minocycline and Ebselen Decrease the Extent of Endothelial Damage and the Width of the Gap Junctions

The effects of ebselen and minocycline on the morphology of the endothelial cells and their gap junctions were studied by electron microscopy. Endothelial cells with early signs of structural changes including cytoplasmic vacuolation (Figure 4A), cuboidal shape, cytoplasmic extensions (Figure 4B and 4C), and detachment from the internal elastic lamina were observed in ebselen-treated and minocycline-treated mice (Figure 4B). However, cellular apoptosis and denudation were not observed in either of the treatment groups compared with untreated mice as we have previously reported.[22]

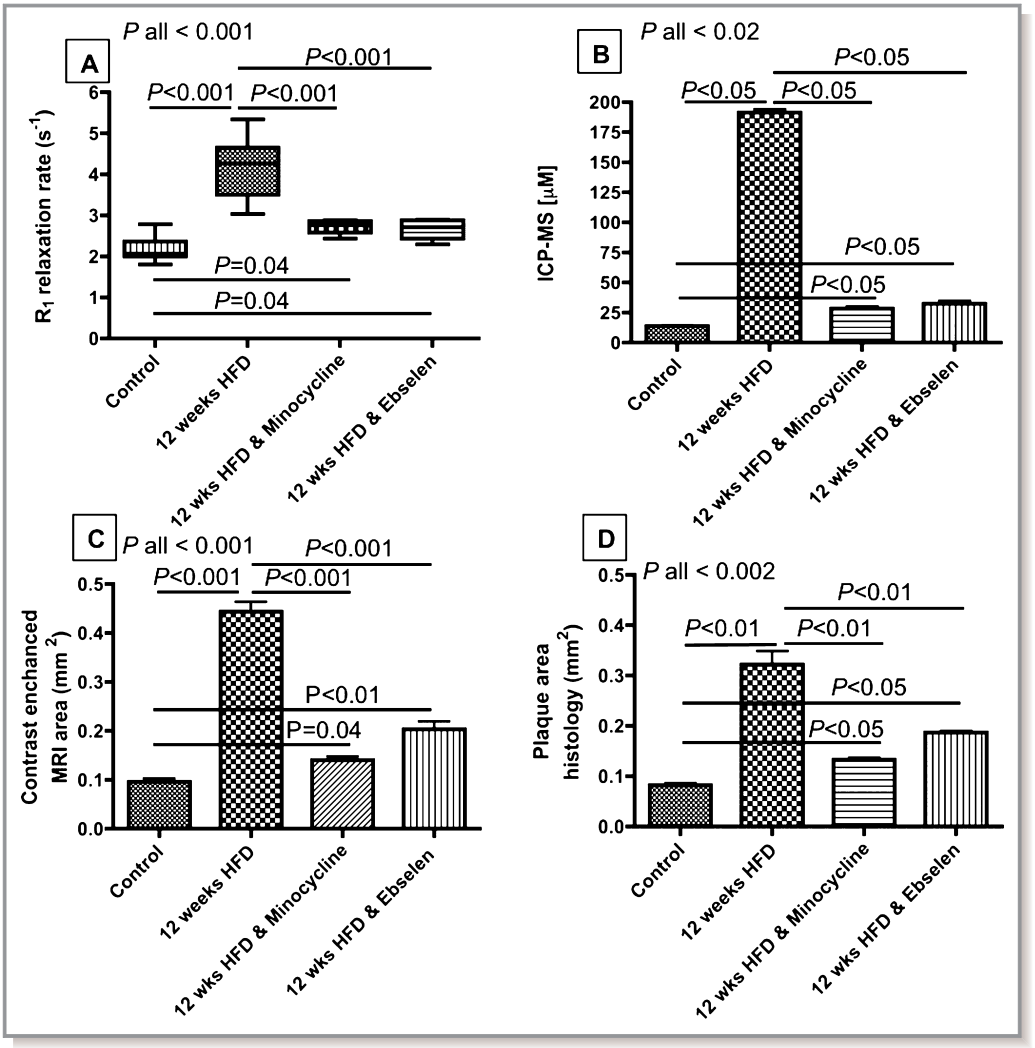

Figure 3. Quantitative MRI and histological analysis. A, R_1 increased in atherosclerotic ApoE$^{-/-}$ mice and decreased in the minocycline- and ebselen-treated animals. B, ICP-MS calculation of gadolinium concentration within the vessel wall. C, Contrast-enhanced vessel wall area. D, Histological assessment of plaque burden. *P* values between groups relate to an ANOVA test with a Bonferroni correction (for A and C) and to a Kruskal–Wallis test followed by a Dunn's post hoc test (for B and D). ANOVA indicates analysis of variance; HFD, high-fat diet; ICP-MS, inductively coupled mass spectrometry; MRI, magnetic resonance imaging.

The majority of endothelial junctions in the ebselen-treated and minocycline-treated groups were characterized by long cytoplasmic overlaps (Figure 4D). However, vacuolated gap junctions with larger gap width between adjacent cells were also observed (Figure 4E and 4F). However, the average gap junction width was smaller in ebselen-treated (56.5±17 nm) and minocycline-treated (42.32±8.4 nm) mice compared with untreated mice (untreated=2400±39 nm), *P*<0.001 (Figure 4G).

Treatment With Minocycline and Ebselen Affects the Tissue Monocyte Subsets

Considering the importance of inflammation in plaque development, we tested whether the effects of minocycline and ebselen on the endothelium decreased the level of plaque inflammation measured as the monocyte/macrophage plaque content (Figure 5). Both interventions significantly reduced the content of total monocytes/macrophages within atherosclerotic brachiocephalic arteries to a similar extent (8.06±3.2% and 7.62±1.73% in ebselen- and minocycline-treated mice, respectively, versus 20.1±2.2% in untreated animals; *P*=0.0067; Figure 5A). Moreover, we observed a significant reduction in Ly-6C^{high} cells infiltrating the arterial wall in both the minocycline (26.42±0.6%) and ebselen (14.07±9.5%) groups compared with untreated-ApoE$^{-/-}$ mice (42.64±6.1%; *P*=0.01) (Figure 5B and 5C). Indeed, the majority of monocytes detected within the brachiocephalic artery of both the ebselen and minocycline groups were Ly6C^{low} cells (85.53±10.33% and 72.68±0.98% in ebselen-

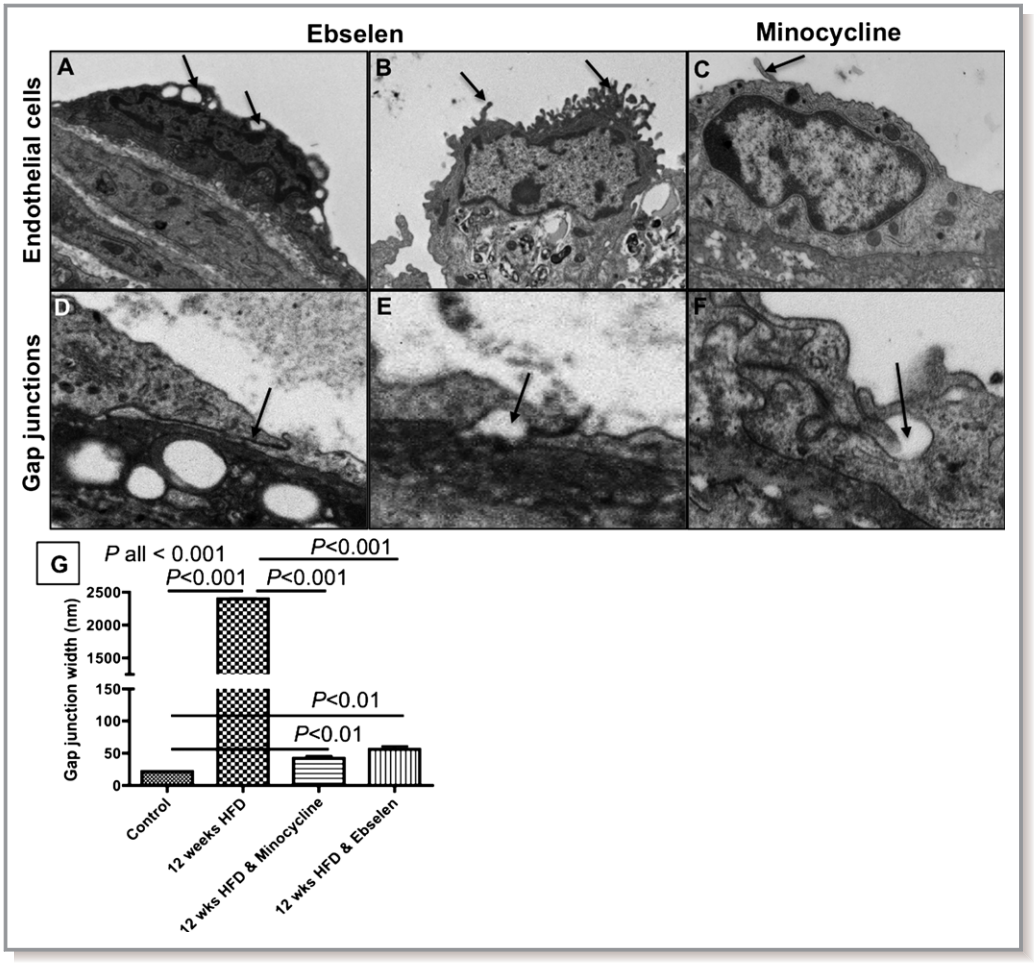

Figure 4. Treatment with minocycline and ebselen decreased the extent of endothelial damage and the width of the junctions. A through C, Examples of structural changes including cytoplasmic vacuolation (A) and cytoplasmic protrusions (B and C) observed in endothelial cells of mice treated with ebselen or minocycline. D through F, Examples of tight junctions with long cytoplasmic overlaps (D) and vacuoles (E and F) observed in mice treated with ebselen or minocycline. G, Junction widths measured by electron microcopy. *P* values between groups relate to a Kruskal–Wallis followed by a Dunn's post hoc test. HFD indicates high-fat diet.

and minocycline-treated mice versus 57.35±6.10% in untreated mice; P=0.03).

Discussion

In this study, we showed that administration of the synthetic antioxidant ebselen and the tetracycline antibiotic minocycline in conjunction with a high-fat diet decreased endothelial permeability and retarded lesion formation in the brachiocephalic artery of atherosclerotic ApoE$^{-/-}$ mice, which could be noninvasively assessed by contrast-enhanced MRI using an albumin-binding contrast agent. Both interventions attenuated the effects of hypercholesterolemia on the structural integrity of the endothelium and the width of the gap junctions as seen by electron microscopy. A reduced content of monocytes/macrophages within the brachiocephalic artery of ebselen- and minocycline-treated animals was also observed compared with untreated mice as seen by flow cytometry. The protective action of ebselen and minocycline on the vascular endothelial barrier is likely to have favorably affected monocyte vascular recruitment and inflammation in treated animals. Indeed, both interventions attenuated the accumulation of pro-inflammatory Ly6C^{high} monocytes within atherosclerotic tissues. Collectively, our data show that leakage of blood albumin into the vessel wall can be used as a surrogate marker to assess vascular permeability and the effectiveness of interventions that aim to restore the integrity of vascular endothelium.

We have recently demonstrated that contrast-enhanced MRI using an albumin-binding contrast agent can be used to noninvasively assess endothelial permeability in vivo.[38] Delayed enhancement, after injection of gadofosveset, correlated with atherosclerosis progression in the brachiocephalic artery of HFD-fed ApoE$^{-/-}$ mice, whereas wild-type and

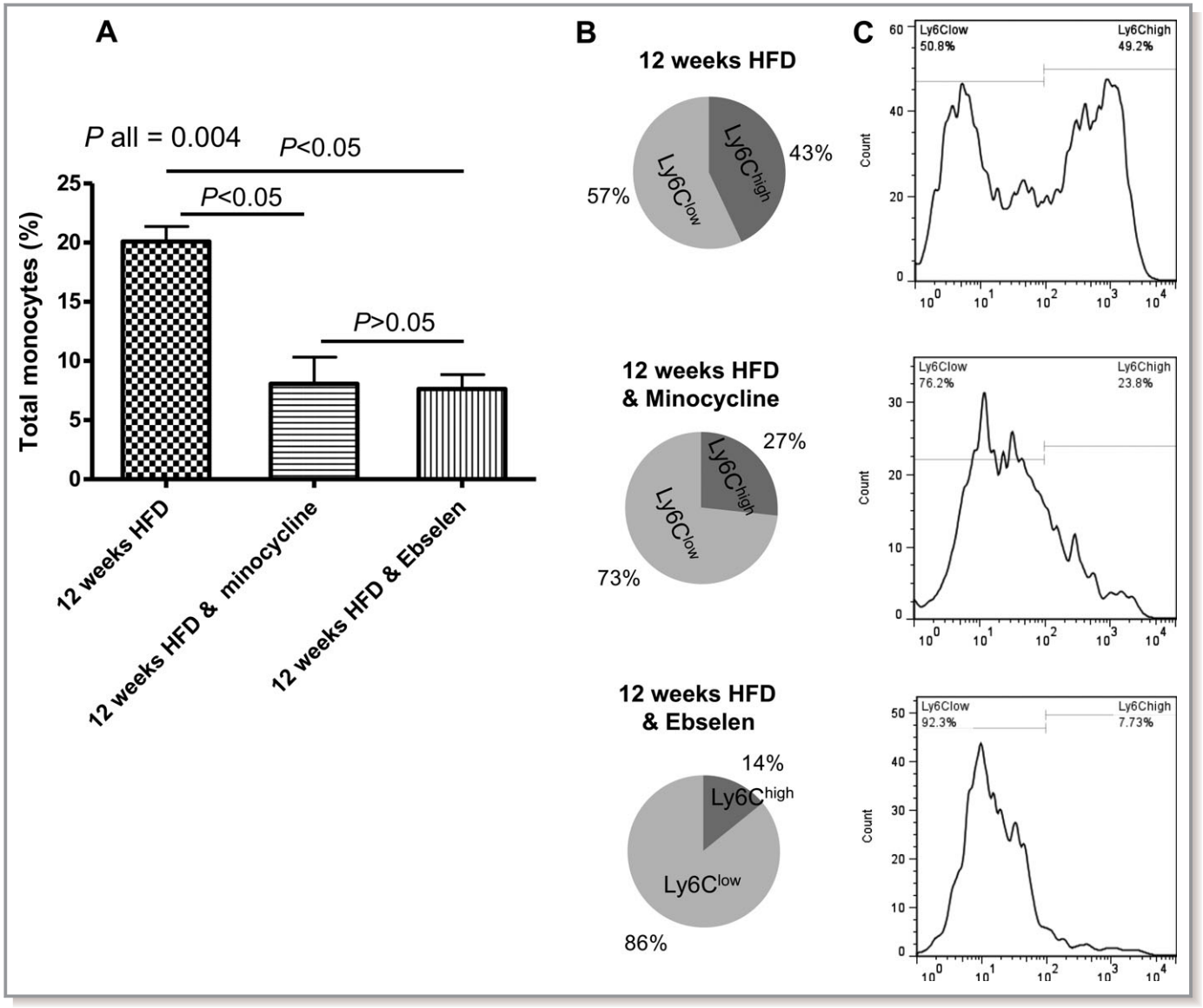

Figure 5. Treatment with minocycline and ebselen reduced the proinflammatory profile of brachiocephalic artery. A, Monocyte characterization in the brachiocephalic artery showing the content of monocytes/macrophages in atherosclerotic tissue of the different groups (monocytes/macrophages were defined as $CD11b^{high}$ $F4/80^{+}$ $CD115^{+}$ Lin^{-} [B220, CD90, Ly6G, NK1.1] cells). B, Illustration of the prevalence of $Ly6C^{high}$ (dark gray) and $Ly6C^{low}$ (light gray) within tissues, expressed as percentage of cells over total monocytes/macrophages. C, Flow cytometer histograms showing typical Ly6C expression in the brachiocephalic artery of the different groups. *P* values between groups relate to a Kruskal–Wallis followed by a Dunn's post hoc test. HFD indicates high-fat diet.

statin-treated $ApoE^{-/-}$ mice showed less uptake. Disease progression was accompanied by a range of morphological changes of the endothelial cells and widening of the cell–cell junctions.

As an extension of our previous work, we investigated the feasibility of MRI using the albumin-binding contrast agent to monitor the efficacy of 2 therapeutic interventions, minocycline and ebselen, on vascular permeability and plaque burden. Our study showed that both interventions retarded lesion formation compared with in untreated mice. Lesion size was decreased by ≈40% to 50%, as measured by DE-MRI and histology, and resulted in lower gadolinium uptake, as indicated by vessel wall relaxivity and ICP-MS measurements. Consistent with our previous results using statin treatment,[38] both minocycline and ebselen attenuated endothelial damage in $ApoE^{-/-}$ mice and decreased gap junction width compared with untreated animals, leading to decreased uptake of gadofosveset within the vessel wall. In both groups endothelial damage was limited to early-stage morphological changes including cytoplasmic vacuolation and protrusions, but no cellular apoptosis and denudation were observed.

Tetracycline derivates, including minocycline and doxycycline, have been shown to reduce neointima formation, MMP activity, and vascular smooth muscle cell migration after

balloon injury of the carotid artery in rats and to inhibit vascular endothelial growth factor–induced MMP-9 mRNA transcription and protein activation in human aortic vascular smooth muscle cells in vitro.[26,42,43] The anti-inflammatory properties of minocycline, including the reduction of interleukin-1 and tumor necrosis factor and inhibition of NF-kB,[44,45] are likely to contribute to the reduction of neointima formation. Similarly to our work, other studies of minocycline treatment in atherosclerotic ApoE$^{-/-}$ mice showed reduction in plaque size and stenosis and decreased frequency and proliferation of plaque smooth muscle cells through a PARP-1- and p27^{Kip1}-dependent mechanism.[28] Moreover, oral administration of minocycline in atherosclerotic rabbits markedly decreased expression of plaque macrophages, MMP-2, and MMP-9.[27]

Ebselen, a peroxynitrite scavenger and antioxidant agent, has been shown to reduce atherosclerotic burden and improve endothelial function in different animal models.[23,24,46] Studies have shown that ebselen reduced diabetes-associated atherosclerosis in ApoE$^{-/-}$ mice.[46] These reductions were accompanied by significantly lower oxidative stress by reducing nitrotyrosine and NADPH oxidase (Nox2) levels; lower expression of inflammatory markers including vascular endothelial growth factor, vascular cell adhesion molecule–1, and MCP-1; and reduced macrophage and vascular smooth muscle cell content. In vitro studies using human aortic endothelial cells showed that ebselen abrogates H_2O_2-induced increases in P-IKK, P-JNK, tumor necrosis factor–α, and Nox2.[24,46] In Zucker diabetic fat rats, a model of type 2 diabetes associated with metabolic syndrome, ebselen prevented premature endothelial cell senescence and improved endothelial dysfunction (improved acetylcholine response).[23] Cellular antioxidant enzymes such as glutathione peroxidase 1 and superoxide dismutase have a central role in the control of reactive oxygen species. A prospective study in patients with suspected coronary artery disease showed that glutathione peroxidase-1 activity was among the strongest univariate predictors of the risk of cardiovascular events.[47] Therefore, bolstering glutathione peroxidase-1 activity by using ebselen treatment might lower the risk of cardiovascular events. Because of its anti-inflammatory properties, ebselen has been used in the treatment of patients with acute ischemic stroke.[48,49] The results of these clinical trials indicate the benefit of ebselen as a neuroprotective agent.

As part of their anti-inflammatory action, we also found that both ebselen and minocycline significantly reduced the content of monocytes/macrophages within the brachiocephalic artery and significantly attenuated the accumulation of pro-inflammatory Ly6C^{high} cells. This common effect on plaque composition can be most likely attributed to the protective action on the endothelial barrier shared by the 2 drugs. It is known that different adhesive molecules expressed by the endothelium selectively recruit distinct monocyte subpopulations within the arterial wall and that recruitment of Ly6C^{high} monocytes mainly occurs under proinflammatory conditions.[50] Unlike Ly6C^{high} monocytes, the Ly6C^{low} subtype appears to have a "patrolling" behavior for the vasculature in mice.[11] Our results suggest that both drugs exerted a significant anti-inflammatory effect at the level of the plaque, which is most likely sustained by a protective action on the vascular endothelium that, in turn, prevents the arterial infiltration of pro-inflammatory Ly6C^{high} monocytes. However, further experiments are needed to define the phenotype of endothelial cells and, as a consequence, the dynamics of monocyte trafficking within atherosclerotic lesions in response to ebselen and minocycline treatments.

Study Limitations

Our study tested the effect of minocycline and ebselen on atherosclerosis when these drugs were administered together with a high-fat diet in a relatively small number of animals. Additional studies with larger sample sizes will be needed to test whether such interventions could promote plaque regression when administered in animals with already-established atherosclerosis. The aim of our study was to test the feasibility of contrast-enhanced MRI using an albumin-binding contrast agent in monitoring the effectiveness of these interventions of vascular permeability and endothelial damage. Therefore, we did not explore the mechanisms by which these drugs exert their atheroprotective effects or their action on monocyte trafficking into lesions. Further studies with larger sample sizes focusing on the cellular and molecular levels are needed to address these issues.

Conclusions

We have demonstrated the feasibility of contrast-enhanced MRI using gadofosveset to noninvasively visualize and quantify the reduction in endothelial permeability and plaque burden in ApoE$^{-/-}$ mice treated with minocycline or ebselen. Both treatments also attenuated hypercholesterolemia-induced monocytosis and had a differential effect on monocyte sunsets. This novel approach may allow screening of the efficacy of different treatments in reducing atherosclerotic disease. As gadofosveset is a clinically approved contrast agent, it may allow translation of our findings to patients with cardiovascular disease.

Sources of Funding

This work was funded by British Heart Foundation grant PG/10/044/28343 (to R.M.B.) and a British Heart Foundation Early Career Development Fellowship (to A.P.). This research

was also supported by the King's BHF Centre of Research Excellence (BHF RE/08/003) and the National Institute for Health Research (NIHR) Biomedical Research Centre at Guy's and St Thomas' NHS Foundation Trust and King's College London.

Disclosures

None.

References

1. Davignon J, Ganz P. Role of endothelial dysfunction in atherosclerosis. *Circulation*. 2004;109:III27–III32.
2. Cai JM, Hatsukami TS, Ferguson MS, Small R, Polissar NL, Yuan C. Classification of human carotid atherosclerotic lesions with in vivo multicontrast magnetic resonance imaging. *Circulation*. 2002;106:1368–1373.
3. Botnar RM, Stuber M, Kissinger KV, Kim WY, Spuentrup E, Manning WJ. Noninvasive coronary vessel wall and plaque imaging with magnetic resonance imaging. *Circulation*. 2000;102:2582–2587.
4. Wasserman BA, Smith WI, Trout HH III, Cannon RO III, Balaban RS, Arai AE. Carotid artery atherosclerosis: in vivo morphologic characterization with gadolinium-enhanced double-oblique MR imaging initial results. *Radiology*. 2002;223:566–573.
5. Yuan C, Kerwin WS, Ferguson MS, Polissar N, Zhang S, Cai J, Hatsukami TS. Contrast-enhanced high resolution MRI for atherosclerotic carotid artery tissue characterization. *J Magn Reson Imaging*. 2002;15:62–67.
6. Maintz D, Ozgun M, Hoffmeier A, Fischbach R, Kim WY, Stuber M, Manning WJ, Heindel W, Botnar RM. Selective coronary artery plaque visualization and differentiation by contrast-enhanced inversion prepared MRI. *Eur Heart J*. 2006;27:1732–1736.
7. Yeon SB, Sabir A, Clouse M, Martinezclark PO, Peters DC, Hauser TH, Gibson CM, Nezafat R, Maintz D, Manning WJ, Botnar RM. Delayed-enhancement cardiovascular magnetic resonance coronary artery wall imaging: comparison with multislice computed tomography and quantitative coronary angiography. *J Am Coll Cardiol*. 2007;50:441–447.
8. Phinikaridou A, Ruberg FL, Hallock KJ, Qiao Y, Hua N, Viereck J, Hamilton JA. In vivo detection of vulnerable atherosclerotic plaque by MRI in a rabbit model. *Circ Cardiovasc Imaging*. 2009;3:323–332.
9. Winter PM, Morawski AM, Caruthers SD, Fuhrhop RW, Zhang H, Williams TA, Allen JS, Lacy EK, Robertson JD, Lanza GM, Wickline SA. Molecular imaging of angiogenesis in early-stage atherosclerosis with alpha(v)beta3-integrin-targeted nanoparticles. *Circulation*. 2003;108:2270–2274.
10. Botnar RM, Perez AS, Witte S, Wiethoff AJ, Laredo J, Hamilton J, Quist W, Parsons EC Jr, Vaidya A, Kolodziej A, Barrett JA, Graham PB, Weisskoff RM, Manning WJ, Johnstone MT. In vivo molecular imaging of acute and subacute thrombosis using a fibrin-binding magnetic resonance imaging contrast agent. *Circulation*. 2004;109:2023–2029.
11. Amirbekian V, Lipinski MJ, Briley-Saebo KC, Amirbekian S, Aguinaldo JG, Weinreb DB, Vucic E, Frias JC, Hyafil F, Mani V, Fisher EA, Fayad ZA. Detecting and assessing macrophages in vivo to evaluate atherosclerosis noninvasively using molecular MRI. *Proc Natl Acad Sci USA*. 2007;104:961–966.
12. Ronald JA, Chen JW, Chen Y, Hamilton AM, Rodriguez E, Reynolds F, Hegele RA, Rogers KA, Querol M, Bogdanov A, Weissleder R, Rutt BK. Enzyme-sensitive magnetic resonance imaging targeting myeloperoxidase identifies active inflammation in experimental rabbit atherosclerotic plaques. *Circulation*. 2009;120:592–599.
13. Makowski MR, Wiethoff AJ, Blume U, Cuello F, Warley A, Jansen CH, Nagel E, Razavi R, Onthank DC, Cesati RR, Marber MS, Schaeffter T, Smith A, Robinson SP, Botnar RM. Assessment of atherosclerotic plaque burden with an elastin-specific magnetic resonance contrast agent. *Nat Med*. 2011;17:383–388.
14. Pedersen SF, Thrysoe SA, Paaske WP, Thim T, Falk E, Ringgaard S, Kim WY. CMR assessment of endothelial damage and angiogenesis in porcine coronary arteries using gadofosveset. *J Cardiovasc Magn Reson*. 2011;13:10.
15. Nguyen PK, Meyer C, Engvall J, Yang P, McConnell MV. Noninvasive assessment of coronary vasodilation using cardiovascular magnetic resonance in patients at high risk for coronary artery disease. *J Cardiovasc Magn Reson*. 2008;10:28.
16. Terashima M, Nguyen PK, Rubin GD, Iribarren C, Courtney BK, Go AS, Fortmann SP, McConnell MV. Impaired coronary vasodilation by magnetic resonance angiography is associated with advanced coronary artery calcification. *JACC Cardiovasc Imaging*. 2008;1:167–173.
17. Hays AG, Hirsch GA, Kelle S, Gerstenblith G, Weiss RG, Stuber M. Noninvasive visualization of coronary artery endothelial function in healthy subjects and in patients with coronary artery disease. *J Am Coll Cardiol*. 2010;56:1657–1665.
18. Lauffer RB, Parmelee DJ, Ouellet HS, Dolan RP, Sajiki H, Scott DM, Bernard PJ, Buchanan EM, Ong KY, Tyeklar Z, Midelfort KS, McMurry TJ, Walovitch RC. MS-325: a small-molecule vascular imaging agent for magnetic resonance imaging. *Acad Radiol*. 1996;3(suppl 2):S356–S358.
19. Caravan P, Cloutier NJ, Greenfield MT, McDermid SA, Dunham SU, Bulte JW, Amedio JC Jr, Looby RJ, Supkowski RM, Horrocks WD Jr, McMurry TJ, Lauffer RB. The interaction of MS-325 with human serum albumin and its effect on proton relaxation rates. *J Am Chem Soc*. 2002;124:3152–3162.
20. Lobbes MB, Miserus RJ, Heeneman S, Passos VL, Mutsaers PH, Debernardi N, Misselwitz B, Post M, Daemen MJ, van Engelshoven JM, Leiner T, Kooi ME. Atherosclerosis: contrast-enhanced MR imaging of vessel wall in rabbit model—comparison of gadofosveset and gadopentetate dimeglumine. *Radiology*. 2009;250:682–691.
21. Lobbes MB, Heeneman S, Passos VL, Welten R, Kwee RM, van der Geest RJ, Wiethoff AJ, Caravan P, Misselwitz B, Daemen MJ, van Engelshoven JM, Leiner T, Kooi ME. Gadofosveset-enhanced magnetic resonance imaging of human carotid atherosclerotic plaques: a proof-of-concept study. *Invest Radiol*. 2010;45:275–281.
22. Phinikaridou A, Andia ME, Protti A, Indermuehle A, Shah A, Smith A, Warley A, Botnar RM. Noninvasive magnetic resonance imaging evaluation of endothelial permeability in murine atherosclerosis using an albumin-binding contrast agent. *Circulation*. 2012;126:707–719.
23. Brodsky SV, Gealekman O, Chen J, Zhang F, Togashi N, Crabtree M, Gross SS, Nasjletti A, Goligorsky MS. Prevention and reversal of premature endothelial cell senescence and vasculopathy in obesity-induced diabetes by ebselen. *Circ Res*. 2004;94:377–384.
24. Chew P, Yuen DYC, Stefanovic N, Pete J, Coughlan MT, Jandeleit-Dahm KA, Thomas MC, Rosenfeldt F, Cooper ME, de Haan JB. Antiatherosclerotic and renoprotective effects of ebselen in the diabetic apolipoprotein E/GPx1-double knockout mouse. *Diabetes*. 2010;59:3198–3207.
25. Baljinnyam E, Hasebe N, Morihira M, Sumitomo K, Matsusaka T, Fujino T, Fukuzawa J, Ushikubi F, Kikuchi K. Oral pretreatment with ebselen enhances heat shock protein 72 expression and reduces myocardial infarct size. *Hypertens Res*. 2006;29:905–913.
26. Pinney SP, Chen HJ, Liang D, Wang X, Schwartz A, Rabbani LE. Minocycline inhibits smooth muscle cell proliferation, migration and neointima formation after arterial injury. *J Cardiovasc Pharmacol*. 2003;42:469–476.
27. Ohshima S, Fujimoto S, Petrov A, Nakagami H, Haider N, Zhou J, Tahara N, Osako MK, Fujimoto A, Zhu J, Murohara T, Edwards DS, Narula N, Wong ND, Chandrashekhar Y, Morishita R, Narula J. Effect of an antimicrobial agent on atherosclerotic plaques: assessment of metalloproteinase activity by molecular imaging. *J Am Coll Cardiol*. 2010;55:1240–1249.
28. Shahzad K, Thati M, Wang H, Kashif M, Wolter J, Ranjan S, He T, Zhou Q, Blessing E, Bierhaus A, Nawroth PP, Isermann B. Minocycline reduces plaque size in diet induced atherosclerosis via p27(Kip1). *Atherosclerosis*. 2011;219:74–83.
29. Geissmann F, Jung S, Littman DR. Blood monocytes consist of two principal subsets with distinct migratory properties. *Immunity*. 2003;19:71–82.
30. Underhill HR, Yuan C, Zhao XQ, Kraiss LW, Parker DL, Saam T, Chu B, Takaya N, Liu F, Polissar NL, Neradilek B, Raichlen JS, Cain VA, Waterton JC, Hamar W, Hatsukami TS. Effect of rosuvastatin therapy on carotid plaque morphology and composition in moderately hypercholesterolemic patients: a high-resolution magnetic resonance imaging trial. *Am Heart J*. 2008;155:584.e581–584.e588.
31. Auffray C, Fogg D, Garfa M, Elain G, Join-Lambert O, Kayal S, Sarnacki S, Cumano A, Lauvau G, Geissmann F. Monitoring of blood vessels and tissues by a population of monocytes with patrolling behavior. *Science*. 2007;317:666–670.
32. Nahrendorf M, Swirski FK, Aikawa E, Stangenberg L, Wurdinger T, Figueiredo JL, Libby P, Weissleder R, Pittet MJ. The healing myocardium sequentially mobilizes two monocyte subsets with divergent and complementary functions. *J Exp Med*. 2007;204:3037–3047.
33. Swirski FK, Libby P, Aikawa E, Alcaide P, Luscinskas FW, Weissleder R, Pittet MJ. Ly-6Chi monocytes dominate hypercholesterolemia-associated monocytosis and give rise to macrophages in atheromata. *J Clin Invest*. 2007;117:195–205.
34. Tacke F, Alvarez D, Kaplan TJ, Jakubzick C, Spanbroek R, Llodra J, Garin A, Liu J, Mack M, van Rooijen N, Lira SA, Habenicht AJ, Randolph GJ. Monocyte subsets differentially employ CCR2, CCR5, and CX3CR1 to accumulate within atherosclerotic plaques. *J Clin Invest*. 2007;117:185–194.

35. Gautier EL, Jakubzick C, Randolph GJ. Regulation of the migration and survival of monocyte subsets by chemokine receptors and its relevance to atherosclerosis. *Arterioscler Thromb Vasc Biol*. 2009;29:1412–1418.
36. Swirski FK, Weissleder R, Pittet MJ. Heterogeneous in vivo behavior of monocyte subsets in atherosclerosis. *Arterioscler Thromb Vasc Biol*. 2009;29:1424–1432.
37. Woollard KJ, Geissmann F. Monocytes in atherosclerosis: subsets and functions. *Nat Rev Cardiol*. 2010;7:77–86.
38. Tacke F, Randolph GJ. Migratory fate and differentiation of blood monocyte subsets. *Immunobiology*. 2006;211:609–618.
39. Wu H, Gower RM, Wang H, Perrard XY, Ma R, Bullard DC, Burns AR, Paul A, Smith CW, Simon SI, Ballantyne CM. Functional role of CD11C+ monocytes in atherogenesis associated with hypercholesterolemia. *Circulation*. 2009;119:2708–2717.
40. Blume U, Orbell J, Waltham M, Smith A, Razavi R, Schaeffter T. 3D T (1)-mapping for the characterization of deep vein thrombosis. *MAGMA*. 2009;22:375–383.
41. Engel DR, Maurer J, Tittel AP, Weisheit C, Cavlar T, Schumak B, Limmer A, van Rooijen N, Trautwein C, Tacke F, Kurts C. CCR2 mediates homeostatic and inflammatory release of GR1(high) monocytes from the bone marrow, but is dispensable for bladder infiltration in bacterial urinary tract infection. *J Immunol*. 2008;181:5579–5586.
42. Yao JS, Chen Y, Zhai W, Xu K, Young WL, Yang GY. Minocycline exerts multiple inhibitory effects on vascular endothelial growth factor-induced smooth muscle cell migration: the role of ERK1/2, PI3K, and matrix metalloproteinases. *Circ Res*. 2004;95:364–371.
43. Bendeck MP, Conte M, Zhang M, Nili N, Strauss BH, Farwell SM. Doxycycline modulates smooth muscle cell growth, migration, and matrix remodeling after arterial injury. *Am J Pathol*. 2002;160:1089–1095.
44. Huang TY, Chu HC, Lin YL, Ho WH, Hou HS, Chao YC, Liao CL. Minocycline attenuates 5-fluorouracil-induced small intestinal mucositis in mouse model. *Biochem Biophys Res Commun*. 2009;389:634–639.
45. Tikka T, Fiebich BL, Goldsteins G, Keinanen R, Koistinaho J. Minocycline, a tetracycline derivative, is neuroprotective against excitotoxicity by inhibiting activation and proliferation of microglia. *J Neurosci*. 2001;21:2580–2588.
46. Chew P, Yuen DY, Koh P, Stefanovic N, Febbraio MA, Kola I, Cooper ME, de Haan JB. Site-specific antiatherogenic effect of the antioxidant ebselen in the diabetic apolipoprotein E-deficient mouse. *Arterioscler Thromb Vasc Biol*. 2009;29:823–830.
47. Blankenberg S, Rupprecht HJ, Bickel C, Torzewski M, Hafner G, Tiret L, Smieja M, Cambien F, Meyer J, Lackner KJ. Glutathione peroxidase 1 activity and cardiovascular events in patients with coronary artery disease. *N Engl J Med*. 2003;349:1605–1613.
48. Masumoto H, Kissner R, Koppenol WH, Sies H. Kinetic study of the reaction of ebselen with peroxynitrite. *FEBS Lett*. 1996;398:179–182.
49. Yamaguchi T, Sano K, Takakura K, Saito I, Shinohara Y, Asano T, Yasuhara H. Ebselen in acute ischemic stroke: a placebo-controlled, double-blind clinical trial. Ebselen Study Group. *Stroke*. 1998;29:12–17.
50. Hristov M, Weber C. Differential role of monocyte subsets in atherosclerosis. *Thromb Haemost*. 2011;106:757–762.